ANTIMICROBIAL AGENTS AND CHEMOTHERAPY, Apr. 2009, p. 1673–1678 Vol. 53, No. 4
0066-4804/09/$08.00+0 doi:10.1128/AAC.01340-08
Copyright © 2009, American Society for Microbiology. All Rights Reserved.

Mutations in Three Distinct Loci Cause Resistance to Peptide Deformylase Inhibitors in *Bacillus subtilis*▽

Yann Duroc, Carmela Giglione, and Thierry Meinnel*

Protein Maturation, Cell Fate and Therapeutics, ISV, UPR2355, Centre National de la Recherche Scientifique, Bât. 23A, 1 avenue de la Terrasse, F-91198 Gif-sur-Yvette Cedex, France

Received 7 October 2008/Returned for modification 11 December 2008/Accepted 20 January 2009

Bacillus subtilis **mutants with resistance against peptide deformylase inhibitors were isolated. All showed a bypass of the pathway through mutations in three genes required for formylation of Met-tRNA^{fMet}, *fmt*, *folD*, and *glyA*. *glyA* corresponds to a yet uncharacterized locus inducing resistance. The bypass of formylation caused robust fitness reduction but was not accompanied by alterations of the transcription profile. A subtle adaptation of the enzymes of the intermediary metabolism was observed.**

In bacteria, all newly synthesized polypeptides transiently carry a formylated N terminus (1, 18, 33). Peptide deformylase (PDF) catalyzes the subsequent removal of the formyl group, and its gene is essential (11, 22, 23). The natural compound actinonin was the first PDF inhibitor (PDFI) characterized (4, 6, 8). Mechanisms causing PDFI resistance involve (i) mutations in the target gene, (ii) bypassing of the formylation pathway, or (iii) efflux of PDFI (4, 9, 10, 15, 17, 19, 20, 25, 31). *Bacillus subtilis* has two functional PDF genes, *def* and *ykrB* (14). The mechanisms of resistance have been studied only in bacteria expressing one active PDF gene. No analysis has approached the implications beyond the fitness cost often associated with PDFI resistance.

To isolate variants resistant to PDFI, 100 μl of an exponential-phase *B. subtilis* culture was plated onto Mueller-Hinton (MH) agar supplemented with 12 μg/ml of actinonin. The plates were incubated for 2 days at 37°C, after which resistant colonies were restreaked and isolated. Cells were also plated

TABLE 1. Mutations, resistance levels, and fitness costs of actinonin-resistant strains

Gene	Identified mutation(s)[a]	No. of independently isolated mutants[b]	MIC of actinonin (μg/ml)[c]	Fitness cost[d]
fmt	Deletion of base pairs 295–639 (codons 99–213; frame conserved); strain Δ*fmt-114*	1	>512	0.48
	Deletion of base pair 119; frameshift (codon 43)	3	192	0.37
	Deletion of base pair 745; frameshift (codon 251)	9	96	0.45
	One base pair insertion at position 745; frameshift (codon 251)	2	96	0.45
	AGA→TGA; R3Stop	1	192	0.44
	CAC→CGC; H108R	1	>512	0.50
	TCC→CCC; S110P	1	>512	0.54
	CCG→CTG; P113L	1	96	0.36
	CGC→TGC; R116C	2*	48	0.45
	CGC→CCC; R116P	1	>512	0.43
	GGT→GAT; G118D	1	>512	0.46
	CCG→CTG; P120L	1	>512	0.34
folD	Deletion of base pairs 199–209 and 219 (codons 67–70 and 73; frame conserved); S71Q, S72Q, and L73P	1	>512	0.50
	Deletion of base pairs 507–518 (codons 172–175; frame conserved)	1	>512	0.41
	GAA→CAA; E17Q	2	192	0.50
	ACG→ATG; T184 M	1	192	0.43
glyA	Deletion of base pairs 661–663 (codon 224; frame conserved)	1*	>512	0.44

[a] Nucleotide and amino acid substitutions and their positions are indicated.
[b] An asterisk (*) indicates that one mutant presented mutations in both genes (*fmt* and *glyA*).
[c] MICs were determined by the microtiter broth dilution technique (26), using MH liquid broth at 37°C after 17 h. The MIC was the lowest antibiotic concentration which prevented growth (i.e., an optical density at 600 nm of <0.01).
[d] The fitness cost corresponds to the ratio of the doubling time of the WT to that of the resistant derivative.

* Corresponding author. Mailing address: Protein Maturation, Cell Fate and Therapeutics, ISV, UPR2355, Centre National de la Recherche Scientifique, Bât. 23A, 1 avenue de la Terrasse, F-91198 Gif-sur-Yvette Cedex, France. Phone: 33169823612. Fax: 33169823607. E-mail: thierry.meinnel@isv.cnrs-gif.fr.

▽ Published ahead of print on 26 January 2009.

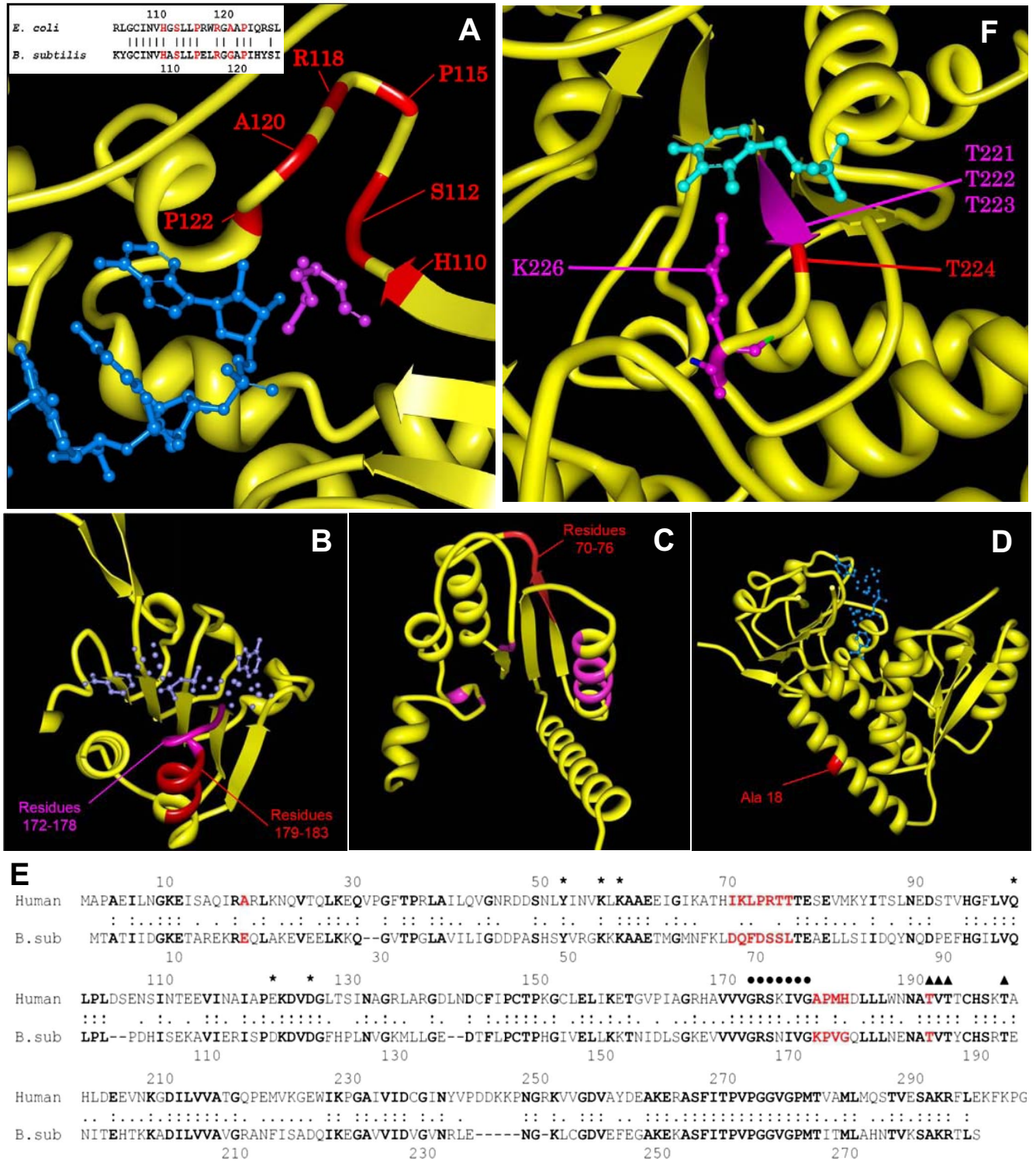

E

```
Human  MAPAEILNGKEISAQIRARLKNQVTQLKEQVPGFTPRLAILQVGNRDDSNLYINVKLKAAEEIGIKATHIKLPRTTTESEVMKYITSLNEDSTVHGFLVQ
B.sub  MTATIIDGKETAREKREQLAKEVEELKKQ--GVTPGLAVILIGDDPASHSYVRGKKKAAETMGMNFKLDQFDSSLTEAELLSIIDQYNQDPEFHGILVQ
Human  LPLDSENSINTEEVINAIAPEKDVDGLTSINAGRLARGDLNDCFIPCTPKGCLELIKETGVPIAGRHAVVVGRSKIVGAPMHDLLLWNNATVTTCHSKTA
B.sub  LPL--PDHISEKAVIERISPDKDVDGFHPLNVGKMLLGE--DTFLPCTPHGIVELLKKTNIDLSGKEVVVVGRSNIVGKPVGQLLLNENATVTYCHSRTE
Human  HLDEEVNKGDILVVATGQPEMVKGEWIKPGAIVIDCGINYVPDDKKPNGRKVVGDVAYDEAKERASFITPVPGGVGPMTVAMLMQSTVESAKRFLEKFKPG
B.sub  NITEHTKKADILVVAVGRANFISADQIKEGAVVIDVGVNRLE-----NG-KLCGDVEFEGAKEKASFITPVPGGVGPMTITMLAHNTVKSAKRTLS
```

FIG. 1. Structural impact of substitutions leading to PDFI resistance in *B. subtilis.* (A) Structural view of *E. coli* formylmethionine transferase complexed with formyl methionyl-tRNA^{fMet} (Protein Data Bank code, 2fmt). The enzyme is represented as a yellow ribbon, formylmethionine as pink solid bonds, and tRNA^{fMet} as blue solid bonds. *E. coli* residues corresponding to mutated *B. subtilis* residues are in red. The inset shows the sequence alignment of the formylmethionine transferase active sites from *E. coli* and *B. subtilis*. Mutated residues are in red. (B through D) Structural view of human methylenetetrahydrofolate dehydrogenase/cyclohydrolase (Protein Data Bank code, 1a4i). The enzyme is represented as a yellow ribbon, the active/binding sites as pink ribbons, and NADP as blue solid bonds. Mutated or deleted residues are in red. (B) NADP binding site and deleted residues downstream. (C) THF binding site and deleted residues. (D) Mutation on Ala18 in the human equivalent of E17Q in *B. subtilis*. (E) Sequence alignment of methylenetetrahydrofolate dehydrogenase/cyclohydrolase from *Homo sapiens* and *B. subtilis*. Mutated or deleted residues are in red. Residues that are conserved between the two sequences are in bold. Residues involved in the THF binding site are marked with an asterisk, residues implied in the NADP binding site are marked with a filled circle,

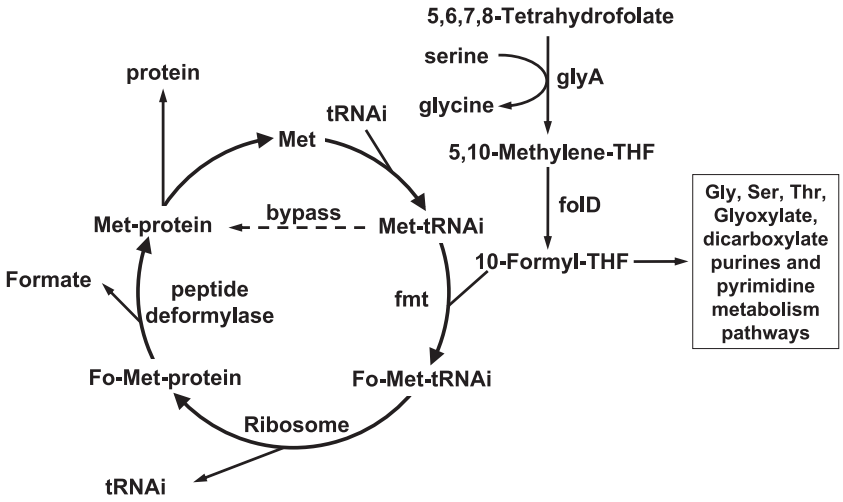

FIG. 2. Translation initiation in bacteria, Met-tRNA formylation, ribosome-mediated protein synthesis, and bypass of the pathway in PDFI-resistant bacteria. tRNAi, $tRNA^{fMet}$.

on minimal medium (MM) agar broth (15 mM ammonium sulfate, 80 mM K_2HPO_4, 45 mM KH_2PO_4, 3.5 mM sodium citrate, 800 μM $MgSO_4$, 0.5% [wt/vol] glucose) supplemented with tryptophan (50 mg/liter) and glycine (25 mg/liter) where indicated below. To assess the fitness cost, growth rates were measured in different broths at 37°C. Cells (10^6) were inoculated into 10 ml of MH medium (Fluka) or in MM without glucose and supplemented with 0.5% (wt/vol) of the indicated carbon source, and then the optical density at 600 nm was measured. In order to identify mutations in open reading frames and/or promoters, given gene loci were amplified with specific primers as shown in Table 1, and the sequences were determined.

The resistance of *B. subtilis* 168 to actinonin was challenged on MH agar at four times the MIC. The resistance rate (10^{-7}) was stable, as repeated streaking on drug-free media did not promote loss of resistance. Resistant strains grew at concentrations much higher than four times the MIC (Table 1). Actinonin-resistant mutants did not show any cross-resistance to other antibiotics but were resistant to other classes of PDFI (7). Both open reading frame and promoter regions of genes (*def*, *ykrB*, *fmt*, and *folD*), the alteration or loss of function of which causes actinonin resistance in other bacteria, were sequenced. No mutation was retrieved in *def* and *ykrB*, and 80% were located in *fmt* (Table 1). Two-thirds of these mutations led to protein sequence alterations, with large deletions due to premature stops, and promoted loss of function of *fmt*. The Δ*fmt-114* strain featured a 114-codon deletion. Single changes involved the catalytic mechanism or binding of the substrates (Table 1; Fig. 1A and B).

Other mutations were located in *folD* (Table 1). *folD* encodes 5,10-methylenetetrahydrofolate dehydrogenase/cyclohydrolase, which produces 10-formyl-tetrahydrofolate (THF), the donor of *N*-formyl to $Met\text{-}tRNA^{fMet}$. Similar mutations have been described only for *Salmonella enterica* (24). The loss of function of *folD* not only bypasses PDF function but also inactivates pathways that use 10-formyl-THF (Fig. 2). When *folD* is inactivated, the strain cannot grow on MM. None of the resistant strains with a *folD* alteration could grow on MM, indicating that the mutations induced loss of function. Several mutations corresponded to deletions. The first deletion identified included residues 67 to 70, with modifications of residues 71 to 73. Structural interpretation was based on the three-dimensional model of FolD (29). The THF binding site is composed of residues conserved in both humans (2) and *B. subtilis* (Fig. 1C to E). The substitutions modify the position of the THF binding site, leading to a dramatic decrease in the reaction efficiency. The second deletion identified (residues 172 to 175) is located next to the NADP binding site $_{165}$GRSNIVG$_{171}$ ($_{172}$GRSKIVG$_{178}$ in humans) (Fig. 1B to E).

There was only one strain carrying an *fmt* mutation that could not grow on MM (Table 1). Given that a nonmutated FolD protein occurred, the origin of the impairment should be due to a mutation upstream in the pathway. One reaction is catalyzed by the *glyA* product, serine hydroxymethyltransferase (Fig. 2), which produces glycine and 5,10-methylene-THF, the substrate of FolD. As growth of the mutant strain on MM was restored in the presence of glycine, this favored an involvement of *glyA*. A deletion of codon 224 in *glyA* was identified. According to the crystallographic model (32), residue 224 lies within the pyridoxal 5′-phosphate (PLP) binding site encompassing residues Thr223 to Lys226 (Fig. 1F). All serine hydroxymethyltransferases have five Thr residues near the active site Lys226, which form the internal glycine-aldimine with PLP

and residues implied in dimer formation are marked with a filled triangle. (F) Structural view of serine hydroxymethyltransferase from *Bacillus stearothermophilus* in complex with pyridoxal-5′-phosphate (Protein Data Bank code, 1kkj). The enzyme is represented as a yellow ribbon, and pyridoxal-5′-phosphate is represented with blue solid bonds. The pyridoxal-5′-phosphate binding site is in pink. A *B. stearothermophilus* residue corresponding to a residue deleted in *B. subtilis* is in red.

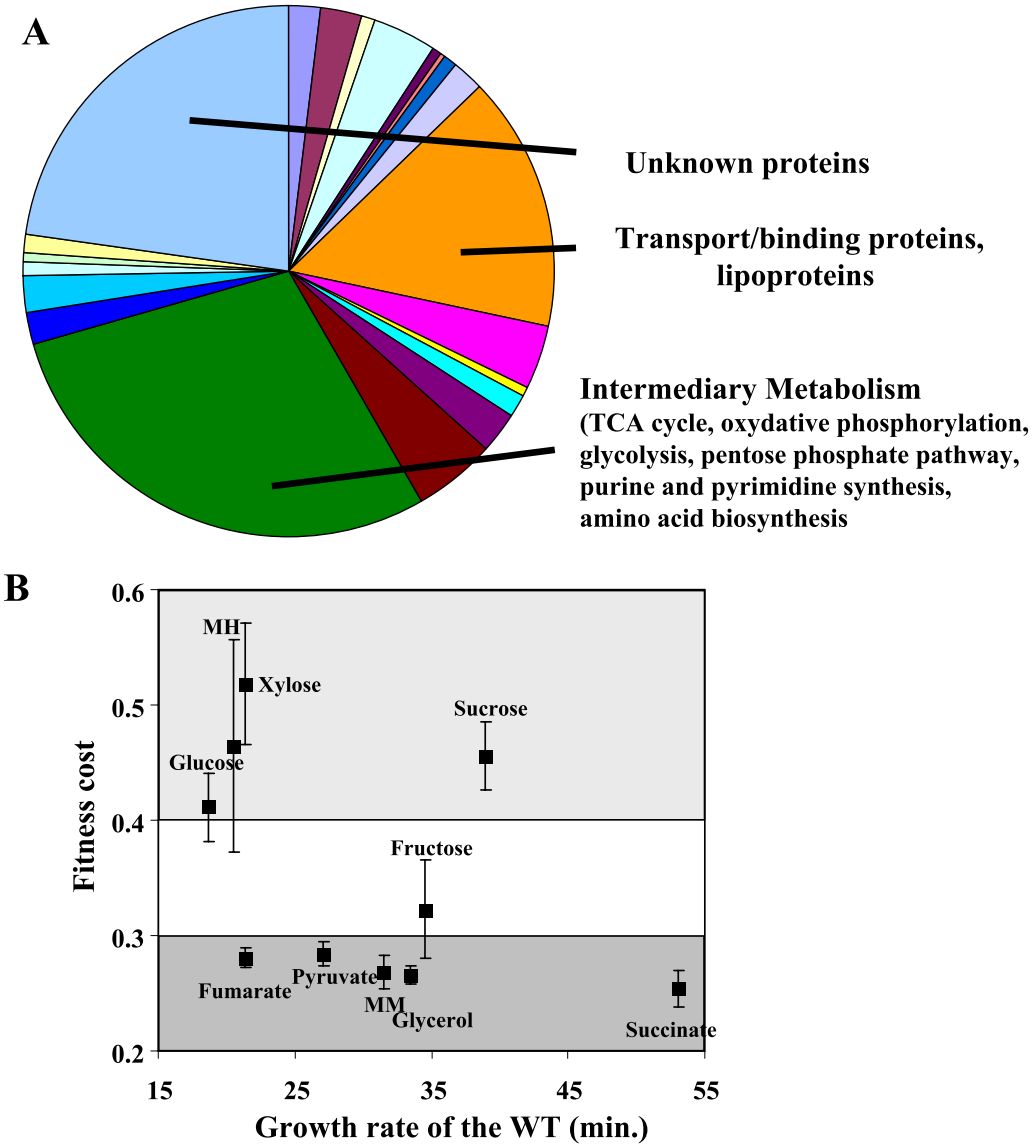

FIG. 3. Physiological differences between WT and PDFI-resistant strains. (A) Gene categories to which the 333 significantly regulated genes belong. Custom compare analysis of the complete *B. subtilis* transcriptome of the WT and resistant strains was performed on microarrays at Eurogentech (Herstaing, Belgium). (B) The doubling times of the WT and Δ*fmt-114* strain were studied in MH medium or MM supplemented with the indicated carbon source. The fitness cost corresponds to the ratio of the doubling time of the WT with that of the resistant derivative. TCA, tricarboxylic acid.

(3, 32). Deletion of Thr224 alters PLP binding (Fig. 1F), inactivating the enzyme. The combination of both the *glyA* and *fmt* mutations confers a higher resistance than that of the strain carrying only the *fmt* mutation. The MIC of actinonin for the first strain was increased 10-fold (Table 1), indicating that (i) the Arg116Cys substitution does not completely inactivate *fmt* and (ii) GlyA modification further completes the bypass of formylation.

All aforementioned mutations inducing PDFI resistance caused fitness costs with two- to threefold reductions in the growth rate in rich media (Table 1). This decrease was higher in MM. This finding confirms that formylation is needed for rapid growth in bacteria (5, 13, 16, 25, 28). However, the fitness cost was less pronounced than in *E. coli* (4, 13, 16). Strains with unambiguous inactivation of the *fmt* gene had distinct doubling times (Table 1). We investigated whether compensatory mechanisms could improve the growth rate by serially passaging several strains in nonselective media through 50 generations. Unlike with PDFI-resistant gram-negative bacteria (12, 21, 25), we were unable to show any improvement in the doubling time. Thus, the fitness burden induced by PDFI resistance is robust. Sequencing of the three *B. subtilis* $tRNA^{fMet}$ genes revealed no modifications or rearrangement, unlike for various gram-positive bacteria (12, 25, 30). Sequencing of the IF_2 gene (*infB*) did not reveal any mutation, although altered expression contributes to fitness cost reduction in *Pseudomonas aeruginosa* (30). Two-dimensional gel electrophoresis of protein accumulation in the Δ*fmt-114* mutant revealed patterns different from those

TABLE 2. Absolute gene regulation in the Δ*fmt-114* mutant

Gene	Absolute gene regulation value[a]	*P* value[b]
atpH	1.11 ± 0.05	0.001
fhuD	1.08 ± 0.03	0.004
pdhA	1.08 ± 0.04	0.001
katA	1.13 ± 0.03	0.001
gtlB	1.10 ± 0.03	0.001
ahpF	1.12 ± 0.05	0.001
thyA	1.04 ± 0.03	0.012
hisC	1.12 ± 0.04	0.001
srfAC	0.92 ± 0.03	0.031

[a] Expressed as the ratio $R = E^{\Delta CT(\mathrm{WT}/\Delta fmt\text{-}114)}{}_{\text{target gene}}/E^{\Delta CT(\mathrm{WT}/\Delta fmt\text{-}114)}{}_{\text{reference gene}}$, where E is PCR efficiency ($10^{-1/\text{slope}}$) and ΔCT is the cycle threshold.
[b] Pairwise fixed reallocation randomization test results.

TABLE 3. Nucleotide sequences of the primers used for PCR amplification

Primer[a]	Sequence (5′ to 3′)
DEF/FMT-F1	ATTTCAATTGATATGAATCCTTATATGATG
DEF/FMT-F2	AAGAGGCATTGCGCCACGGCAT
DEF/FMT-R1	ACCGATTTCAGCAGCAGGTTGCTGTATGCC
DEF/FMT-R2	ATCGGAGCACCGCCGCGCAGTT
YKRB-F	TGCATACGCTGTCAAAGAATTGGGCCTTTT
YKRB-R	CGGGTCCTGTCCCATGCATCCTGTTAATAT
FOLD-F	TATATACTTTGTCAGCGCTGAGACGGTCAC
FOLD-R	AGTTTGTAAACGGGGTTCTTTCTAACATTAA
GLYA-F1	TCGTACCTGTATTTTCATTCCGTATATATG
GLYA-F2	CTTGTTACGAAAGGTTTTTCAGGATCATAT
GLYA-R1	AGCCTCGGTTCAGCTCATGTGACATTGGCG
GLYA-R2	ATCTGTTTTGACAAATAAGTACGCAGAAGG
ATPH-F	GGAGTCGCTTCACTGAGAATCA
ATPH-R	CTTACGCTGCCGTCATAAATCC
FHUD-F	CTGCAGGCTACAAAGCTGACAA
FHUD-R	GCGAAGTCAGGGAGCTTCTCTA
PDHA-F	AGGGAGAAGTCGTGAATGAAGC
PDHA-R	GAGATAGAGCGTTGGTCAAGCA
KATA-F	GTGAACTTGGCTCTGCTGACAC
KATA-R	CCGACGATGTCGTAGTTTCCTT
GTLB-F	CAGCTGATGAGCTAAAGGAGCA
GTLB-R	AGTCGCGTCCTTCGATTAAGAG
AHPF-F	GGCAAGTCTTGAAGAGCATGTG
AHPF-R	GCACCTGTTGAAAGGATCACTG
THYA-F	CAATCCATCTTCACGCAGACAC
THYA-R	CTCAAGGTGGAGTTTCCCATGT
HISC-F	GCCGCTCTTAAGCAAGTATTCC
HISC-R	AATTCCGTATCCGACTCTGAGC
SRFAC-F	CTGATGGCTTGCAGGATGTAAC
SRFAC-R	GCATAGCTTGTATGACGGCAAG
RPLL-F	CTTTAAGCTCTTCAGCTTCTTCTTTAGC
RPLL-R	GTTGTACGTGAAATCACTGGTCTTG

[a] F, forward; R, reverse.

for the wild type (WT), indicative of adaptation mechanisms associated with formylation bypass. Comparison of the transcriptome of the Δ*fmt-114* strain with that of the WT revealed that the expression of a small number of genes was altered by more than twofold, with 308 upregulated and 25 downregulated (Fig. 3A).

To confirm the expression changes between the WT and the Δ*fmt-114* strain, quantitative PCR experiments were performed, using *rplL* for normalization (Table 2). Total RNA was isolated from 5-ml portions of bacterial samples by using an RNeasy minikit (Qiagen) as described by the manufacturer. Genomic DNA was eliminated by RNase-free DNase I treatment during the isolation procedure. cDNAs were prepared, using the SuperScript III First-Strand system. We subjected 5 μg of total RNA to reverse transcription, using random hexamers. The cDNA was then amplified by PCR, using specific oligonucleotides. Real-time PCR was optimized with a LightCycler FastStart DNA Master Sybr green kit (Roche) for each primer pair shown in Table 3 (the amplification efficiency was always >90%), using a standard cDNA. Each cDNA sample was independently quantified three times, with two technical replicates of each. Relative transcript levels were calculated by using the relative expression software tool (REST) (27). Expression of the *rplL* gene was used as a reference for the determination of induction levels. No evidence for regulation was observed for genes involved in translation. The gene categories showing the highest changes corresponded to genes encoding functions of the intermediary metabolism (Fig. 3A). These categories produce the most-abundant proteins, which suggests that energetic metabolism limits growth and is the root of the fitness cost. Thus, in the tested conditions, (i) there is no global change of gene expression and (ii) the adaptation mechanisms involved are subtle.

To understand whether those adaptation mechanisms could be mediated by the growth rate and/or substrate utilization, we tested if fitness could depend on the growth medium. Growth was performed on either MH medium or MM. The growth rate with several carbon sources varied from 18.6 to 53.1 min. There was no correlation between growth rate and fitness cost, and two types of fitness defects could be detected (Fig. 3B). In rich medium or in MM supplemented with a mono- or disaccharide, the doubling time was reduced by twofold. With carboxylic acids such as pyruvate, the growth rate was reduced fourfold. We concluded that sugar utilization in the context of the Δ*fmt-114* strain is more effective than that of carboxylic acids. This difference reflects the limited efficiency of the tricarboxylic cycle/oxidative phosphorylation and the pentose phosphate pathway in the context of the mutant strain, possibly compensating for the overall reduced translation efficiency of these major proteins induced by the loss of formylation of Met-tRNA^{fMet}.

Y.D. was supported by Centre National de la Recherche Scientifique (CNRS, France) and by a postdoctoral grant from the Région Ile-de-France. This work was supported by CNRS and by grant ANR-06-MIME-010 from the Agence Nationale de la Recherche (ANR, France).

REFERENCES

1. **Adams, J. M., and M. Capecchi.** 1966. *N*-Formylmethionine-sRNA as the initiator of protein synthesis. Proc. Natl. Acad. Sci. USA **55:**147–155.
2. **Allaire, M., Y. Li, R. E. MacKenzie, and M. Cygler.** 1998. The 3-D structure of a folate-dependent dehydrogenase/cyclohydrolase bifunctional enzyme at 1.5 Å resolution. Structure **6:**173–182.
3. **Angelaccio, S., S. Pascarella, E. Fattori, F. Bossa, W. Strong, and V. Schirch.** 1992. Serine hydroxymethyltransferase: origin of substrate specificity. Biochemistry **31:**155–162.
4. **Apfel, C. M., H. Locher, S. Evers, B. Takács, C. Hubschwerlen, W. Pirson, M. G. P. Page, and W. Keck.** 2001. Peptide deformylase as an antibacterial drug target: target validation and resistance development. Antimicrob. Agents Chemother. **45:**1058–1064.
5. **Arnold, H. H.** 1977. Initiation of protein synthesis in bacillus subtilis in the presence of trimethoprim or aminopterin. Biochim. Biophys. Acta **476:**76–87.
6. **Boularot, A., C. Giglione, I. Artaud, and T. Meinnel.** 2004. Structure-activity relationship and therapeutic potential of peptide deformylase inhibitors. Curr. Opin. Investig. Drugs **5:**809–822.

7. **Boularot, A., C. Giglione, S. Petit, Y. Duroc, R. A. Sousa, V. Larue, T. Cresteil, F. Dardel, I. Artaud, and T. Meinnel.** 2007. Discovery and refinement of a new structural class of potent peptide deformylase inhibitors. J. Med. Chem. **50:**10–20.
8. **Chen, D. Z., D. V. Patel, C. J. Hackbarth, W. Wang, G. Dreyer, D. C. Young, P. S. Margolis, C. Wu, Z. J. Ni, J. Trias, R. J. White, and Z. Yuan.** 2000. Actinonin, a naturally occurring antibacterial agent, is a potent deformylase inhibitor. Biochemistry **39:**1256–1262.
9. **Clements, J. M., R. P. Beckett, A. Brown, G. Catlin, M. Lobell, S. Palan, W. Thomas, M. Whittaker, S. Wood, S. Salama, P. J. Baker, H. F. Rodgers, V. Barynin, D. W. Rice, and M. G. Hunter.** 2001. Antibiotic activity and characterization of BB-3497, a novel peptide deformylase inhibitor. Antimicrob. Agents Chemother. **45:**563–570.
10. **Dean, C. R., S. Narayan, J. Richards, D. M. Daigle, S. Esterow, J. A. Leeds, H. Kamp, X. Puyang, B. Wiedmann, D. Mueller, H. Voshol, J. van Oostrum, D. Wall, J. Koehn, J. Dzink-Fox, and N. S. Ryder.** 2007. Reduced susceptibility of *Haemophilus influenzae* to the peptide deformylase inhibitor LBM415 can result from target protein overexpression due to amplified chromosomal *def* gene copy number. Antimicrob. Agents Chemother. **51:**1004–1010.
11. **Giglione, C., M. Pierre, and T. Meinnel.** 2000. Peptide deformylase as a target for new generation, broad spectrum antimicrobial agents. Mol. Microbiol. **36:**1197–1205.
12. **Guillon, J.-M., S. Heiss, J. Soutourina, Y. Mechulam, S. Laalami, M. Grunberg-Manago, and S. Blanquet.** 1996. Interplay of methionine tRNAs with translation elongation factor Tu and translation initiation factor 2 in *Escherichia coli*. J. Biol. Chem. **271:**22321–22325.
13. **Guillon, J.-M., Y. Mechulam, J.-M. Schmitter, S. Blanquet, and G. Fayat.** 1992. Disruption of the gene for Met-tRNA$_f^{Met}$ formyltransferase severely impairs growth of *Escherichia coli*. J. Bacteriol. **174:**4294–4301.
14. **Haas, M., D. Beyer, R. Gahlmann, and C. Freiberg.** 2001. YkrB is the main peptide deformylase in *Bacillus subtilis*, a eubacterium containing two functional peptide deformylases. Microbiology **147:**1783–1791.
15. **Hackbarth, C. J., D. Z. Chen, J. G. Lewis, K. Clark, J. B. Mangold, J. A. Cramer, P. S. Margolis, W. Wang, J. Koehn, C. Wu, S. Lopez, I. G. Withers, H. Gu, E. Dunn, R. Kulathila, S. H. Pan, W. L. Porter, J. Jacobs, J. Trias, D. V. Patel, B. Weidmann, R. J. White, and Z. Yuan.** 2002. *N*-Alkyl urea hydroxamic acids as a new class of peptide deformylase inhibitors with antibacterial activity. Antimicrob. Agents Chemother. **46:**2752–2764.
16. **Harvey, R. J.** 1973. Growth and initiation of protein synthesis in *Escherichia coli* in the presence of trimethoprim. J. Bacteriol. **114:**309–322.
17. **Kosowska-Shick, K., K. L. Credito, G. A. Pankuch, B. DeWasse, P. McGhee, and P. C. Appelbaum.** 2007. Multistep resistance selection and postantibiotic-effect studies of the antipneumococcal activity of LBM415 compared to other agents. Antimicrob. Agents Chemother. **51:**770–773.
18. **Marcker, K., and F. Sanger.** 1964. *N*-Formyl-methionyl-S-RNA. J. Mol. Biol. **8:**835–840.
19. **Margolis, P., C. Hackbarth, S. Lopez, M. Maniar, W. Wang, Z. Yuan, R. White, and J. Trias.** 2001. Resistance of *Streptococcus pneumoniae* to deformylase inhibitors is due to mutations in *defB*. Antimicrob. Agents Chemother. **45:**2432–2435.
20. **Margolis, P. S., C. J. Hackbarth, D. C. Young, W. Wang, D. Chen, Z. Yuan, R. White, and J. Trias.** 2000. Peptide deformylase in *Staphylococcus aureus*: resistance to inhibition is mediated by mutations in the formyltransferase gene. Antimicrob. Agents Chemother. **44:**1825–1831.
21. **Marliere, P., R. Mutzel, and D. Mazel.** November 2005. Descendant of bacteria devoid of N-terminal formylation useful for the production of proteins and peptides. U.S. patent 6,962,807 B2.
22. **Mazel, D., S. Pochet, and P. Marliere.** 1994. Genetic characterization of polypeptide deformylase, a distinctive enzyme of eubacterial translation. EMBO J. **13:**914–923.
23. **Meinnel, T., and S. Blanquet.** 1994. Characterization of the *Thermus thermophilus* locus encoding peptide deformylase and methionyl-tRNA$_f^{Met}$ formyltransferase. J. Bacteriol. **176:**7387–7390.
24. **Nilsson, A.** 2005. Resistance adaptation to novel selection pressure. Ph.D. thesis. Stockholm University, Stockholm, Sweden.
25. **Nilsson, A. I., A. Zorzet, A. Kanth, S. Dahlstrom, O. G. Berg, and D. I. Andersson.** 2006. Reducing the fitness cost of antibiotic resistance by amplification of initiator tRNA genes. Proc. Natl. Acad. Sci. USA **103:**6976–6981.
26. **Pearson, R. D., R. T. Steigbigel, H. T. Davis, and S. W. Chapman.** 1980. Method of reliable determination of minimal lethal antibiotic concentrations. Antimicrob. Agents Chemother. **18:**699–708.
27. **Pfaffl, M. W., G. W. Horgan, and L. Dempfle.** 2002. Relative expression software tool (REST) for group-wise comparison and statistical analysis of relative expression results in real-time PCR. Nucleic Acids Res. **30:**e36.
28. **Samuel, C. E., C. L. Murray, and J. C. Rabinowitz.** 1972. Methionine transfer ribonucleic acid from folate-sufficient and folate-deficient *Streptococcus faecalis* R. J. Biol. Chem. **247:**6856–6865.
29. **Shen, B. W., D. H. Dyer, J. Y. Huang, L. D'Ari, J. Rabinowitz, and B. L. Stoddard.** 1999. The crystal structure of a bacterial, bifunctional 5,10-methylene-tetrahydrofolate dehydrogenase/cyclohydrolase. Protein Sci. **8:**1342–1349.
30. **Steiner-Mosonyi, M., C. Creuzenet, R. A. Keates, B. R. Strub, and D. Mangroo.** 2004. The *Pseudomonas aeruginosa* initiation factor IF-2 is responsible for formylation-independent protein initiation in *P. aeruginosa*. J. Biol. Chem. **279:**52262–52269.
31. **Teo, J. W., P. Thayalan, D. Beer, A. S. Yap, M. Nanjundappa, X. Ngew, J. Duraiswamy, S. Liung, V. Dartois, M. Schreiber, S. Hasan, M. Cynamon, N. S. Ryder, X. Yang, B. Weidmann, K. Bracken, T. Dick, and K. Mukherjee.** 2006. Peptide deformylase inhibitors as potent antimycobacterial agents. Antimicrob. Agents Chemother. **50:**3665–3673.
32. **Trivedi, V., A. Gupta, V. R. Jala, P. Saravanan, G. S. Rao, N. A. Rao, H. S. Savithri, and H. S. Subramanya.** 2002. Crystal structure of binary and ternary complexes of serine hydroxymethyltransferase from *Bacillus stearothermophilus*: insights into the catalytic mechanism. J. Biol. Chem. **277:**17161–17169.
33. **Webster, R. E., D. L. Engelhardt, and N. D. Zinder.** 1966. In vitro protein synthesis: chain initiation. Proc. Natl. Acad. Sci. USA **55:**155–161.